

# Simulation of time-dependent ionization processes in acetylene

Thomas Schnappinger<sup>1,\*</sup>, Christian Burger<sup>2,3</sup>, Atia Atia-Tul-Noor<sup>4,5</sup>, Han Xu<sup>4,5</sup>, Philipp Rosenberger<sup>2,3</sup>, Nida Harem<sup>4,5</sup>, Robert Moshhammer<sup>6</sup>, Robert T. Sang<sup>4,5</sup>, Boris Bergues<sup>2,3</sup>, Michael S. Schuurman<sup>7</sup>, Igor Litvinyuk<sup>4,5</sup>, Matthias F. Kling<sup>2,3</sup>, and Regina de Vivie-Riedle<sup>1</sup>

<sup>1</sup>Department of Chemistry, Ludwig-Maximilians-Universität München, D-81377 Munich, Germany

<sup>2</sup>Department of Physics, Ludwig-Maximilians-Universität München, D-85748 Garching, Germany

<sup>3</sup>Max Planck Institute of Quantum Optics, D-85748 Garching, Germany

<sup>4</sup>Australian Attosecond Science Facility, Griffith University, Nathan, Queensland 4111, Australia

<sup>5</sup>Centre for Quantum Dynamics, Griffith University, Nathan, Queensland 4111, Australia

<sup>6</sup>Max Planck Institute of Nuclear Physics, D-69117 Heidelberg, Germany

<sup>7</sup>National Research Council of Canada, 100 Sussex Dr, Ottawa, Ontario, Canada

**Abstract.** We have investigated nuclear dynamics in bound and dissociating acetylene molecular ions in a time-resolved reaction microscopy experiment with a pair of few-cycle pulses. Different ionization processes were observed for acetylene. These time-dependent ionization processes are simulated using semi-classical on-the-fly dynamics revealing the underlying mechanisms.

## 1 Enhanced ionization and r-dependent tunnel ionization

The interaction of molecules with intense laser pulses typically results in ionization. In small molecules like acetylene nuclear motion is induced thereby and subsequent chemical reactions can be initiated [1]. During bond elongation enhanced ionization (EI) can occur, if the molecules interact with a second laser pulse [2]. In a simple diatomic molecule this process can be described as follows: While the internuclear distance increases the potential barrier for the ionization decreases leading to an increase of the ionization rate. At a critical distance the barrier becomes lowest and the rate for EI maximal. For larger molecular system this process is naturally more complex as multiple degrees of freedom opening various pathways for enhanced ionization. Beside EI also r-dependent tunnel ionization can occur in bound states. In this joined experimental and theoretical work we are investigating both ionization processes (EI and r-dependent tunnel ionization) in acetylene ions.

We focused on two ionization scenarios displayed in Fig 1. for the pump-probe experiment. In the scenario a), the pump pulse ionizes acetylene into bound states of the cation (for example the  $X^2\Pi_u$  state as seen in Fig 1. a), forming oscillating vibrational wave packets. The nuclear dynamics is probed by a next ionization step in which also a dissociating state of the dication is populated. Here, the products of deprotonation ( $C_2H^+$  and  $H^+$ ) or isomerization ( $CH_2^+$  and  $C^+$ ) are detected. In the scenario b), the pump pulse

---

\* Corresponding author: [thomas.schnappinger@cup.uni-muenchen.de](mailto:thomas.schnappinger@cup.uni-muenchen.de)

directly populates a dissociative state of the dication ( $A^3\Pi_u$  as displayed in Fig 1. b). The probe pulse enables further ionization, generating a dissociative quadruple charged state, which fragments by Coulomb explosion to  $C^+$ ,  $C^+$ ,  $H^+$  and  $H^+$ .

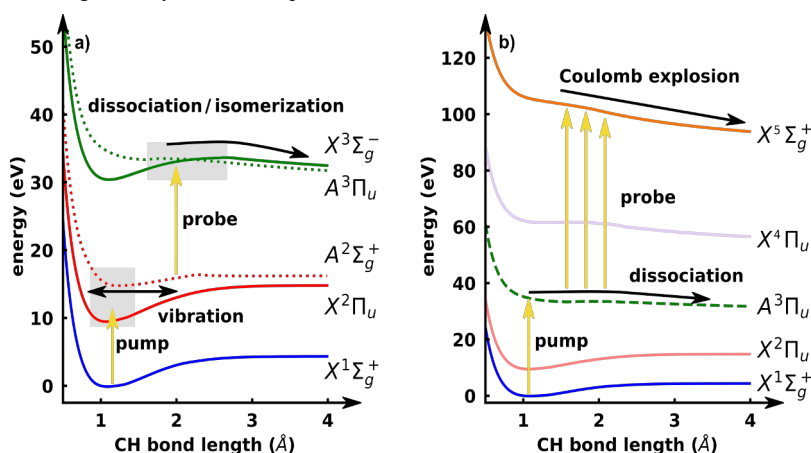


**Fig. 1.** Potential energy curves for various states in neutral and various charged states of acetylene as a function of CH-bond length. In scenario a) the pump pulse ionizes the molecule into a bound cation state (here the  $X^2\Pi_u$  state) and a subsequent probe pulse populates a dissociative dication state (here the  $A^3\Pi_u$  state). In scenario b), the pump pulse directly populates the dissociative dication state ( $A^3\Pi_u$ ), and the probe pulse induces fragmentation from a quadruple charged molecular state.

## 2 Computational Methods

The time-dependent ionization processes are calculated using a combination of non-adiabatic on-the-fly simulations and *ab-initio* calculations of ionization rates. For all these calculations the Complete Active Space Self-Consistent Field method (CASSCF) was employed. To simulate both scenarios shown in Fig 1. trajectories were propagated in the ground state of the acetylene cation ( $X^2\Pi_u$ ) and the first excited state of the dication ( $A^3\Pi_u$ ). For 20 typical trajectories the ionization probability (hereafter called rate) was calculated with the ansatz described in Refs. [3,4]. In this ansatz, a quantum chemical calculation for a given molecular geometry with and without a static electric field is performed. Based on the obtained two electronic densities the tunnelling rate can be extracted. For acetylene the highest three occupied orbitals are included to build up the electronic densities. The static ansatz is benchmarked against the TDRIS approach and shows qualitatively good agreement.

## 3 Interpretation of the ionization mechanisms

Enhanced ionization for dissociating acetylene is observed in scenario b) (see Fig 1.), where initially a dissociative dication state ( $A^3\Pi_u$ ) is populated by the pump pulse. To investigate the subsequent nuclear dynamics, the kinetic energy release (KER) and the number of the ionic fragments created by the probe pulse is analysed experimentally. In Fig 2. a), the ionization yield of the dissociative quadruple charged state is shown as a function of KER and delay between pump and probe pulses. The one-dimensional representation depicted in Fig 2. b) represents the integrated signal (red) and average KER (black) for

dissociating molecules. When inspecting the change in KER with delay time, its decrease from about 45 eV to 22 eV and almost no constant KER contribution was detected.

This indicates that all molecules detected undergo dissociation in the intermediately populated  $A^3\Pi_u$  state. With respect to the ionization yield (red), we could observe a clear indication of enhanced ionization in acetylene. After a few fs, the ionization yield increases between 10 fs and 40 fs. For delays beyond 40 fs, the ionization yield decreases again. In figure 2. c), the calculated average KER (black) and the average ionization rate (red) are shown as a function of the simulation time (only the first 60 fs are displayed, and the ionization rate is calculated every femtosecond). The KER decrease from about 45 eV to 22 eV within the first 30 fs. In this time scale all trajectories show the dissociation of one proton. Along this dissociation process the ionization rates starts to peak after 10 fs at an average CH-bond length of 2.2 Å which corresponds well to the experimentally observed starting position of the yield enhancement. Compared to the experiment the time scale of the dynamics simulation is too fast, since the CASSCF method overestimate the steepness of the potential energy. But overall the experimental results are reproduced well. We will also show our first results on the r-dependent tunnel ionization demonstrating the dominant role of the CC-stretching vibration and the isomerization process.

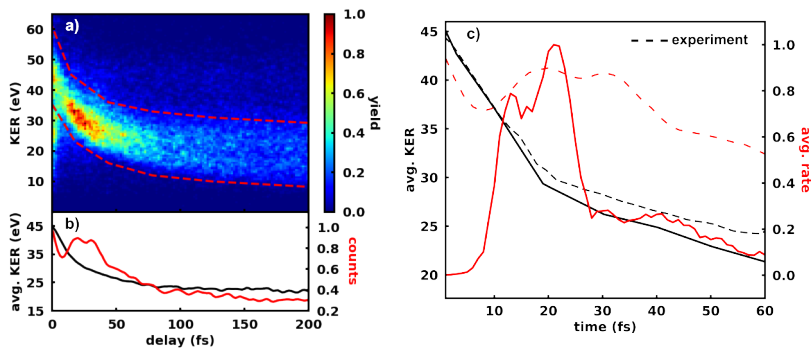


**Fig. 2.** a) Ionization yield of the dissociative quadruple charged state as a function of KER and delay time. b) The one-dimensional plot represents the normalized KER-integrated signal including all counts within the dissociative area (red line) and the average KER of the dissociative events as a function of the delay time (black line). c) Theoretical calculations of the average KER (black) and the average ionization rate (red) as a function of the simulation time (experimental results are shown in dotted lines).

## References

1. M. Kübel, R. Siemering, C. Burger, N. G. Kling, H. Li, A. S. Alnaser, B. Bergues, S. Zhrebtssov, A. M. Azzee, I. Ben-Itzhak, R. Moshammer R. de Vivie-Riedle, and M. F. Kling, *Phys. Rev. Lett.* **116**, 193001 (2016)
2. J. Wu, M. Meckel, L. P. H. Schmidt, M. Kunitski, S. Voss, H. Sann, H. Kim, T. Jahnke, A. Czasch, and R. Dörner, *Nat. Commun.* **3**, 1113 (2012)
3. P. von den Hoff, I. Znakovskaya, S. Zhrebtssov, M. F. Kling, and R. de Vivie-Riedle, *Appl. Phys. B Lasers Opt.* **98**, 659666 (2010)
4. B. Jochim, R. Siemering, M. Zohrabi, O. Voznyuk, J. B. Mahowald, D. G. Schmitz, K. J. Betsch, B. Berry, T. Severt, N. G. Kling, T. G. Burwitz, K. D. Carnes, M. F. Kling, I. Ben-Itzhak, E. Wells, and R. de Vivie-Riedle, *Sci. Rep.* **7**, 4441 (2017)